Thermal Stability and Crystalline of Electrospun Polyamide 6/Organo-Montmorillonite Nanofibers

Qi Li,[1,2] Dawei Gao,[1] Qufu Wei,[1] Mingqiao Ge,[1] Weimin Liu,[2] Lejiang Wang,[2] Keqin Hu[2]

[1]*Key Laboratory of Eco-Textiles, Ministry of Education, Jiangnan University, Wuxi 214122, China*
[2]*Zhejiang Institute of Modern Textile Industry, Keqiao 312030, Zhejiang, China*

Received 12 December 2008; accepted 27 December 2009
DOI 10.1002/app.32017
Published online 29 March 2010 in Wiley InterScience (www.interscience.wiley.com).

ABSTRACT: This research is mainly to investigate the thermal and crystalline differences between polyamide 6/montmorillonite (PA6/MMT) and polyamide 6/organo-montmorillonite (PA6/O-MMT) nanofibers, which were both prepared by electrospinning under the same process conditions. The structures of PA6/MMT and PA6/O-MMT nanofibers were observed by scanning electrical microscope. It was identified that the interval between O-MMT clays was increased in the PA6 matrix compared to that of MMT, which was detected by X-ray diffraction (XRD). The thermal properties of PA6 nanofibers contained O-MMT particles were more efficient than PA6/MMT nanofibers, that was verified using thermal gravimetric analysis. The crystalline properties of the electrospun nanofibers was investigated using differential scanning calorimeter and it was found that the degree of crystallinity in the PA6 nanofibers loaded with O-MMT was much higher than PA6/MMT and PA6 nanofibers. © 2010 Wiley Periodicals, Inc. J Appl Polym Sci 117: 1572–1577, 2010

Key words: atomic force microscopy (AFM); fibers; morphology; nanolayers; thermal properties

INTRODUCTION

In the past decade, polymer layered silicate nanocomposites (PLSN) have received considerable attention in fundamental research and industry exploitation due to their potential to display synergistically advanced properties with only small amounts (e.g., 1–3 wt %) of clay loading. Among the silicate clays, the most common octahedral smectite is montmorillonite, which has two siloxane tetrahedral sheets sandwiching an aluminum octahedral sheet (with high diameter-thickness ratio of about 200). Among all the systems investigated, PLSN have presented drastically enhancing properties of thermal stability,[1,2] tensile/flexural strength,[3] flame retardancy, and barrier property.[4] However, the majority of investigations on PLSN have focused on the molded materials[1–3,5] with few researches reported closely on the formation and properties of PMSN nanofibers via electrospinning.[3,6,7]

Successful pioneering work on these nanocomposites was conducted on the polyamide 6/montmorillonite (PA6/MMT) clay system,[8] attracting intensive researches on PA6/MMT fibers, films, plastic applications, and especially composite nanofibers. It has been found that the tensile properties of nanofibers containing OMMT clays were dramatically improved and the Young's modulus and ultimate strength of electrospun nanocomposite fibrous mats were also improved up to 70% and 30%, respectively, when compared to nylon-6 electrospun mats.[3] It was also found that the dynamic water adsorption was also improved when the clays were added into the nanofibers by 1–2%.[6]

Nevertheless, most of the current research work was concentrated on melting extruding progress,[1,7] not only in the molded materials but also in composite nanofibers.[3,5] In this article, a conventional composite technique was applied. MMT and O-MMT were firstly dispersed in the *N*,*N*-dimethyl formamide respectively and then compounded with PA6, which was dissolved in formic acid in advance. The composite solutions were electrospun and formed PA6/MMT and polyamide 6/organo-montmorillonite (PA6/O-MMT) composite nanofibers. The dispersion exfoliation of O-MMT in DMF solution was detected using atomic force microscope (AFM) for the first time. The further dispersion and exfoliation of clays were examined by XRD. The formation and

Correspondence to: Q. Wei (qfwei@jiangnan.edu.cn).
Contract grant sponsor: Program for New Century Excellent Talents in University; contract grant number: NCET-06-0485.
Contract grant sponsor: Specialized Research Fund for the Doctoral Program of Higher Education; contract grant number: 20090093110004.
Contract grant sponsor: Program for Innovative Team of Jiangsu Province (2009-9).

structure of electrospun fibers was investigated using scanning electrical microscope (SEM). The differences in thermal stability and crystalline properties of the composite nanofibers loaded with different clays were also investigated and discussed.

EXPERIMENTAL

Materials

The montmorillonite without modification and organo-montmorillonite, which was modified by ion exchange reaction using hexadecyl trimethyl ammonium bromide, both purchased from Zhejiang Fenghong Clay Chemicals Co. The average thickness of the particle was less than 25 nm, and the ratio of diameter to thickness was about 200. Polyamide 6 (intrinsic viscosity was 2.8 dL/g), 99.5% *N*,*N*-dimethyl formamide (DMF) and 88% formic acid were all used as received.

Preparation of composite nanofibers

All the nanofillers and PA6 pellets were dried for 8 h at 80°C under vacuum to remove moisture. The MMT clay slurry was prepared by dispersing MMT (4 g) dry power into DMF (48.52 mL) solvent using magnetic stirring for 30 min until the powder uniformly dispersed in the DMF solvent. Meanwhile, the O-MMT slurry was made using the same procedure. Furthermore, 15 wt % of polyamide 6 dissolved in formic acid was also prepared. The prepared clay slurry was then put into the polyamide 6 solution, which was mixed in an ultrasonic bath for another 50 min.

The labratory electrospinning apparatus consisted of a syringe, a needle, and a high voltage power in which a positive voltage (14 kV) was applied to the polymer solution though the needle attached to the syringe. The solution jet was formed by electrostatic force, when the electrical potential increased to 14 kV. The nanofibers in a nonwoven form were collected on an aluminum foil. The ejection rate of the solution was set at 0.2 mL/h, which was adjusted by a syringe pump. The distance between the needle tip and the collector was 10 cm.

Structural characterization of nanofibers

Scanning electrical microscope (SEM) Quanta 200 was applied to examine the structural differences of the nanofiber nonwovens. The samples of the electrospun nanofibers were coated with a thin layer of gold by sputtering before the SEM imaging. The diameters of the nanofibers were measured by ImageJ software based on the SEM images and 100 nanofibers were randomly selected from each sample.

The thickness of O-MMT clays in the slurry was detected using AFM (Benyuan CSPM 4000). The sample was prepared using newly released mica, on which there was clay slurry with ultra-low concentration. Scanning was carried out in tapping mode under ambient conditions. Furthermore, to detect the interval variation of clays via electrospinning, X-ray diffraction (XRD) patterns were performed on the 1 mm thick films using a Japan Rigaku D/Max-Ra rotating anode X-ray diffractometer equipped with a Cu-Kα tube and Ni filter ($\lambda = 0.1542$ nm).

Thermal stability and crystallinity

Thermal gravimetric analyses (TGA) were conducted on a TGA50H thermo- analyzer instrument from 25 to 700°C using a linear heating rate of 10°C/min under nitrogen atmosphere. All the samples were pretreated for 1 h using vacuum drying with heated air, and measured in a sealed alumina pan with a mass of about 5(±0.5) mg. Finally, crystalline properties of different composite nanofibers were examined by a differential scanning calorimeter (DSC 822e, Mettler-Toledo, Switzerland) using a linear heating rate of 5°C/min under nitrogen atmosphere. The samples were also pretreated for 1 h using vacuum drying with heated air.

RESULTS AND DISCUSSION

Fibrous structure of composite nanofibers

The structures of fibrous nonwoven webs made of the electrospun nanofibers were investigated using SEM. All the nanofibers were collected randomly on the aluminum foil forming fibrous webs as shown in Figure 1. The images indicate that the electropun nanofibers have varying diameters in the fibrous web. The average diameter of the sample electropun from neat PA6 solution is around 262 nm, but exhibits some extremely fine and ruptured nanofibers as indicated in Figure 1(A). Furthermore, the average diameter of composite nanofibers loaded with 2 wt % MMT is decreased to nearly 133.8 nm, while the diameter of the composite nanofibers contained 2 wt % O-MMT nanofillers is dramatically decreased approximately to 82.5 nm with the existence of more superfine and ruptured fibers, as revealed in Figure 1(B,C), respectively. The viscoelastic behavior of the polymer solution plays an importance role as the electrostatic forces applied to the electrospun solutions are fixed in this work. Lower surface tension and viscosity of the spinning solution contribute to the formation of the narrowly distributed ultrafine nanofibers.[6] Meanwhile, the conductivity of the PA6

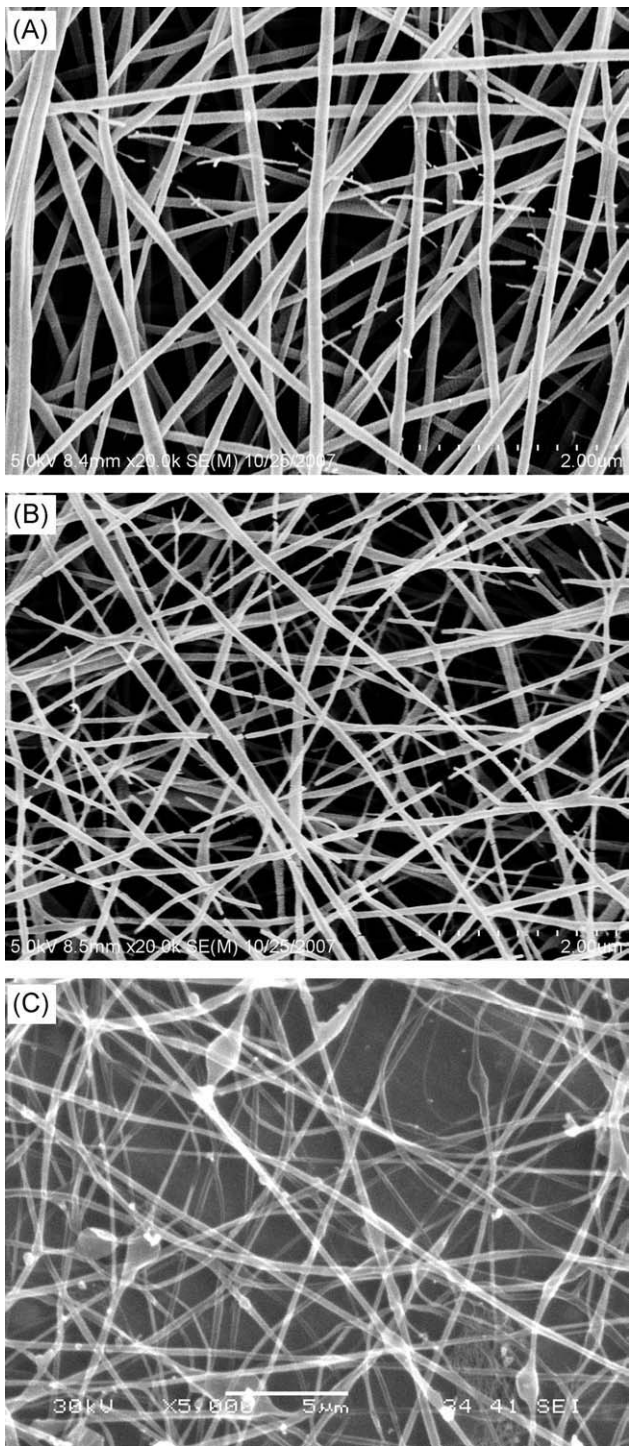

Figure 1 SEM images of (A) PA6 nanofibers, (B) PA6/O-MMT, and (C) PA6/MMT composite nanofibers.

solution is another major factor affecting the morphology and diameter of the electrospun PA6 nanofibers. The addition of quaternary ammonium used to modify MMT clays increases the charge density in ejected jets and thus, stronger stretching forces are imposed to the jets due to the self repulsion of the excess charges under the electrostatic field, resulting in a substantially straighter shape and smaller diameter of electrospun nanofibers.[7]

It is clearly observed from the SEM images in Figure 1 that the electrospun nanofibers made of PA6 and PA6/O-MMT solutions present very homogeneous fibers without bead-on-string structures at the same concentration, while the image of the electrospun nanofibers from PA6/MMT solution show many bead-on-string, sumpling, and nubby structures. In the PA6/MMT spinning solution, hydrophilic MMT clays are hard to fully exfoliate, but aggregate which also changes the solution homogeneity resulting in lower viscosity and heterogeneous conductivity. However, the MMT clays modified using quaternary ammonium, which has wide clay interval and lipophilic, promote the PA6 molecular chains to enter the interval between the clays, so all the O-MMT particles could be completely and homogeneously spread in the spinning solution. Moreover, there is less ruptured fiber observed in PA6/MMT structure, while some extremely thin nanofibers in the PA6 and PA6/O-MMT samples are broken during the sampling progress.

AFM analysis of clays in the DMF solution

The image in Figure 2 reveals the structures of the O-MMT clays in the DMF solution. The clays show different shapes and sizes in the DMF solution. The AFM image is depicted with black lines, which are marked with number 1, 2, 3, and 4, respectively, as shown in Figure 2. The average thickness of the O-MMT clays is about 25 nm, but the AFM Imager Software reveals the thickness of O-MMT in the DMF is 1.80 nm, 3.39 nm, 1.80 nm, 1.93 nm successively for the marked locations. The AFM

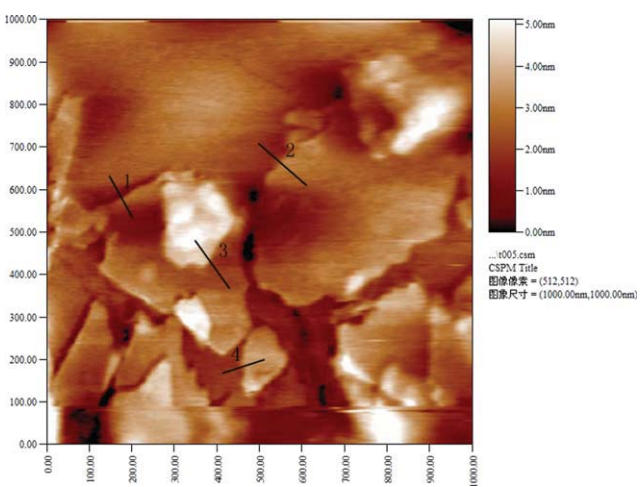

Figure 2 AFM image of O-MMT clay in the DMF solution. [Color figure can be viewed in the online issue, which is available at www.interscience.wiley.com.]

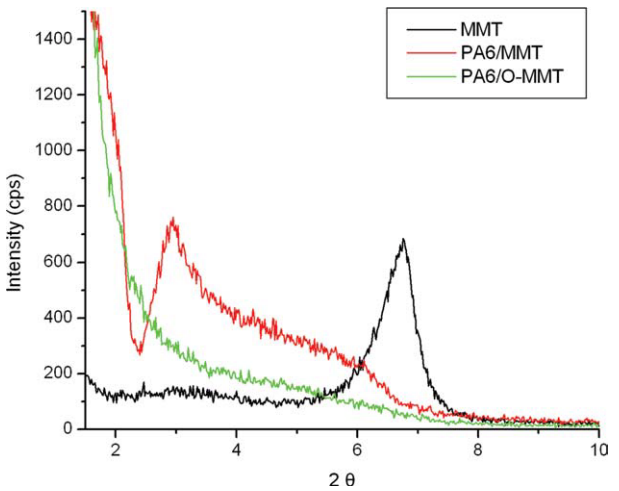

Figure 3 XRD patterns of the composite nanofibers. [Color figure can be viewed in the online issue, which is available at www.interscience.wiley.com.]

observations also indicate the average surface roughness of the O-MMT clays in the DMF solution is about 0.54 nm.

It is clearly observed that some clays are exfoliated to single-ply structure, but quite a part of clays exist in multi-ply structure, as shown in Figure 2. This observation proves that the way of dispersing O-MMT clays into DMF solvent using magnetic stirring, would be only helpful to the preliminary dissociation of montmorillonite.

XRD analysis

The results of the XRD analysis are shown in Figure 3. It can be observed that the MMT and PA6/MMT nanofibers show clear peaks in the XRD patterns. The peaks indicate the distance between the adjacent MMT lamellar structure, being approximately in MMT powders $2\Theta = 6.75°$, $d = 13.2$ Å (1.32 nm) according to Bragg's law. The peak of PA6/MMT shows the reflection of MMT shifting to lower angle ($2\Theta = 2.94°$) corresponds to $d = 30.5$ Å (3.05 nm). A reduction in the diffraction angle is related to increasing in silicate layer distance. In other words, the silicate layers in PA6/MMT composite nanofibers are exfoliated into the larger space.

The XRD patterns in Figure 3 also clearly reveal the disappearance of the peak in PA6/O-MMT composite nanofibers. It is suggested that the OMMT layers are adequately exfoliated in the polymer matrix. In other word, PA macromolecules intercalate into the silicate layers, and the disordered and delaminated OMMT layers in the PA6/O-MMT nanofibers shows no peak in this region due to the loss of structural regularity of the layers. No more diffraction peaks are visible in the XRD pattern of exfoliated structures, which confirms the results in the reference.[9]

Thermal stability

The TGA-scanned results of the samples are shown in Figure 4. Figure 4 reveals the three phases of degradation that occur in the samples. Although all the samples display the similar degradation progress, but in the term of the onset of thermal stability, PA6/O-MMT and PA6/MMT composite nanofibers are not enhanced compared to that of pure PA6 nanofiber. The onset degradation (3 wt % weight loss) of composite nanofibers reduces from 405.2°C for the neat PA6 nanofibers to 394.8°C for the PA6/MMT nanofibers and 382.5°C for the PA6/O-MMT nanofibers. It is possible that the organic solvent in the nanofibers loaded with montmorillonite clay is the most unstable and will degrade first. It is understandable that there is some solvent trapped in the nanofibers during the fiber spinning. In addition, the evaporation of organic solvent is not only occurs in the composite nanofibers, but also between the clay layers.

Furthermore, the PA6 nanofibers exhibits the least thermal stability, and the PA6/O-MMT shows the best thermal stability among samples, which can be proved by TGA data as shown in Figure 4. For instance, the yield of charred residue at 700°C is increased from 5.5 wt % for the neat PA6 nanofibers, to 10.6 wt % for the PA6/MMT nanofibers and 13.5 wt % for the PA6/O-MMT nanofibers. The increased amount of the charred residue can verify the increasing thermal stability of the PA6 composite nanofibers. The increased charred residue amount

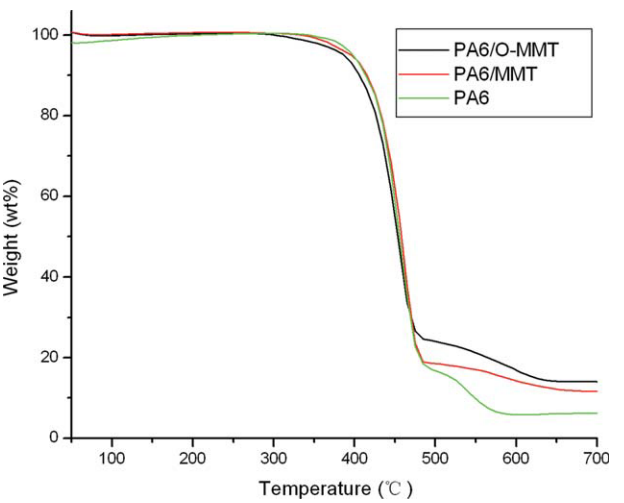

Figure 4 Thermal stability of PA6, PA6/MMT, and PA6/O-MMT composite nanofibers. [Color figure can be viewed in the online issue, which is available at www.interscience.wiley.com.]

contributes to the improved thermal stability of the PA6 composite nanofibers.

The TGA results evidently suggest that the thermal stability of PA6 nanofibers is enhanced by loading silicate layers, and the thermal stability of the PA6 loaded with O-MMT is better than that loaded with MMT because of the homogeneous dispersion of layered silicates, which results in oxygen and heat permeability reductions in the PA 6 matrix during the heating scans.[4]

Crystalline properties

PA6 has been reported to exhibit two main crystalline forms, namely α and γ. The α form is thermodynamically stable, but the γ form is kinetically favored, and they are usually associated with two different melting temperatures, 221°C and 215°C, respectively.[2] Furthermore, the form can transform to the γ form at elevated temperatures. The image in Figure 5 shows the DSC curves of composite nanofibers. It can be found that the melting peak temperature of PA6 is 219°C. It is also observed that the melting peak temperature of PA6/MMT is around 222.29°C and the melting peak temperature of PA6/O-MMT is similar at 221.95°C, which both are slightly higher than that of the neat PA6 nanofibers. Therefore, this indicates that the α crystals are dominated in PA6 composite nanofibers regardless of the type of clay layers and the crystal structures in composite nanofibers are slightly more thermally stable.

Figure 5 clearly indicates that the PA6/MMT and PA6/O-MMT composite nanofibers have only one melting peak while PA6 nanofibers have two melting peaks. A small endothermic shoulder associated with melting of the γ form of nylon-6 crystals is observed in all heating scans at a temperature lower than the main melting point, which has also been reported in the literature.[3] The width of the melting peak presents the distribution dimension of the crystal particles.[2] The crystallization of the neat PA6 and the composite PA6 nanofibers conducted by DSC scans can be calculated from the ratio of the testing heat of fusion (ΔH_f) to the heat of the completely crystalline forms of neat PA6 (ΔH_f) with the value of 190.9 J/g. The degree of crystallinity of the samples is list in Table I. It can be noted that the composite nanofibers have a higher crystallization than the neat PA6 nanofibers, which generally is between 20 and 30%. During the process of crystallization, smaller particles are more apt to nucleate, accelerating the crystallization of PA6 composites nanofibers and increasing the degree of crystallization. As is shown in the SEM images, the structure of PA6/O-MMT nanofibers is much straighter than that of PA6/MMT and most of the O-MMT is distributed in the fibers. So the degree of crystallinity for the PA6 nanofibers loaded O-MMT is much higher than PA6/MMT nanofibers.

TABLE I
Crystal Data

	PA6	PA6/MMT	PA6/O-MMT
ΔH_f (J/g)	48.7	56.73	67.9
X (%)	25.5	29.7	36.4

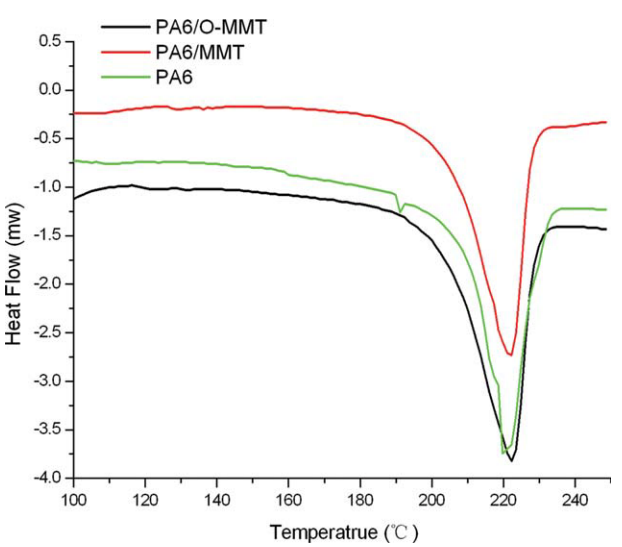

Figure 5 DSC chart of PA6, PA6/MMT, and PA6/O-MMT composite nanofibers. [Color figure can be viewed in the online issue, which is available at www.interscience.wiley.com.]

CONCLUSION

This study has explored the structural characteristics, thermal stability, and crystalline properties of the electrospun PA6, PA6/MMT, and PA6/O-MMT composite nanofibers. In the electrospinning progress, the variation of surface tension, viscosity, and conductivity of spinning solution, led to the decrease in nanofiber diameters. Particularly, the PA6/MMT nanofibers not only appeared nanofibers but also many bead-on-string, sumpling, and nubby structures. It was also identified that the interval of O-MMT was increased in the PA6 matrix compared to MMT. It was found that the degree of crystalline of the PA6 nanofibers loaded O-MMT was much higher than that of PA6/MMT nanofibers, which showed higher degree of crystalline than PA6 nanofibers.

References

1. Chattopadhyay, D. K.; Aswini, M. K.; Sreedhar, B.; Raju, K. V. S. N. Polym Degrad Stab 2006, 91, 1837.

2. Sun, L.; Yang, J. T.; Lin, G. Y.; Zhong, M. Q. Mater Lett 2007, 61, 3963.
3. Li, L.; Bellan, L. M.; Craighead, H. G. Polymer 2006, 47, 6208.
4. Chiu, F. C.; Fu, S. W.; Chuang, W. T.; Sheu, H. S. Polymer 2008, 49, 1015.
5. Yudina, V. E.; Divouxb, G. M.; Otaigbe, J. U.; Svetlichnyi, V. M. Polymer 2005, 46, 10866.
6. Li, Q.; Wei, Q. F.; Wu, N.; Cai, Y. B.; Gao, W. D. J Appl Polym Sci 2007, 11, 3535.
7. Choi, J. S.; Lee, S. W.; Jeong, L.; Bae, S. H.; Chan, M. B.; Youk, J. H.; Parka, W. H. Int J Biol Macromol 2004, 34, 249.
8. Hasegawa, N.; Okamoto, H.; Kato, M.; Norio Sata, A. Polymer 2003, 44, 2933.
9. Hao, X. Y.; Gai, G. S.; Liu, J. P.; Yang, Y. F.; Zhang, Y. H.; Nan, C. W. Mater Chem Phys 2006, 96, 34.